JPE 5-1-5

Direct Torque Control System of a Reluctance Synchronous Motor Using a Neural Network

Min-Huei Kim†

†Yeungnam College of Science and Technology, Republic of Korea

ABSTRACT

This paper presents an implementation of high performance control of a reluctance synchronous motor (RSM) using a neural network with a direct torque control. The equivalent circuit in a RSM, which considers iron losses, is theoretically analyzed. Also, the optimal current ratio between torque current and exiting current is analytically derived. In the case of a RSM, unlike an induction motor, torque dynamics can only be maintained by controlling the flux level because torque is directly proportional to the stator current. The neural network is used to efficiently drive the RSM. The TMS320C31 is employed as a control driver to implement complex control algorithms. The experimental results are presented to validate the applicability of the proposed method. The developed control system shows high efficiency and good dynamic response features for a 1.0 [kW] RSM having a 2.57 ratio of d/q.

Keywords: Direct Torque Control, Neural Network, Reluctance Synchronous Motor, High Performance Control

1. Introduction

The need for high performance has drawn industrial attention to losses that occur due to inefficient and imprecise control of motors. The desire for better performance has led to a greater focus on improvement of materials and optimization of design strategies. However, efficiency and precision control can also be improved by intervening in the operational principle of motors. Several simple and effective control methods have been proposed in order to minimize the losses and to improve dynamic responses[5],[9].

Manuscript received June 21, 2004; revised October 23, 2004.
† Corresponding Author: mhkim@ync.ac.kr, Dept. of Automatic Electrical Eng., Yeungnam College of Science.& Technology, Tel: +82-53-650-9263, Fax: +82-53-624-4736.

Recently, neural network (NN) control, which can map non-linear relations between input and output signals, and direct torque control (DTC), which is simple and provides good dynamic response, have gotten a lot of attention. In particular, a lot of research has been done to apply these controls to induction and synchronous motor drives.

In general, DTC can be divided into two methods, the constant flux method and the variable flux method. The commonly used constant flux method keeps the exciting current constant regardless of the load.

At lighter loads, maximum efficiency will be achieved by reducing the exciting current. Consequently, there is an optimum exciting current which will most efficiently provide the specified torque and speed [1].

The reluctance synchronous motor (RSM) has gained an increasing popularity in various industry applications. RSM's have recently been offered by some researchers as

a viable alternative to induction, synchronous and switched reluctance machines in medium-performance drive applications. This has been made possible by limiting some traditional RSM drawbacks, such as poor power factor and low-torque density which are related to the limited saliency ratio obtained by using a conventional rotor design. The RSM has certain advantages over other types of ac machines. Unlike other types of ac machines, the RSM's mechanical simplicity and robust structure allow it to operate at high speeds in high temperature environments. In addition, the absence of rotor joule and iron rotor loss in the case of a sinusoidally distributed m.m.f. results in better exploitation of stator structures and a colder rotor, which is preferred in certain applications. Furthermore, these motors require little maintenance. These advantages make the RSM very attractive for a wide variety of low and high speed applications and also in high dynamic performance drives [3]-[10].

In this paper, an efficiency optimized current angle condition in the RSM that minimizes the copper and the iron loss is derived based on the equivalent circuit model of the machine. From this mathematical analysis, the optimal flux reference can be obtained. However, because the RSM's inductance is changed nonlinearly as current, it is used in the NN. The NN's used in this paper are trained off-line to map the optimal flux reference. In order to implement the neural network and DTC algorithm, the TMS320C31 DSP board is used. The proposed algorithm allows the electromagnetic losses in variable speed/torque drives to be reduced while maintaining good dynamic response. Experimental results are presented to validate the proposed algorithm.

2. Reluctance Synchronous Motors

The RSM has a stator winding similar to those of a three-phase induction motor and a rotor designed with appreciably different values of the reluctance on the direct and quadrature axes. The RSM has advantages over both the induction and synchronous motor [3]. The electromagnetic torque production of the RSM depends on the ratios of L_d and L_q inductance(saliency ratio). In early RSM's, the d-axis and q-axis inductance ratios could not exceed more than 2:1 resulting in a larger frame size than an equivalent induction motor. However, developments in power electronics have led to variable speed drives and improvements in design have allowed a higher saliency ratio. Indeed, ratios L_d/L_q (8~20) have been reported and there are many different saliency ratios versus rotor types. In this paper, a flux barrier rotor was used to reduce cost and allow mass production [3],[4].

The vector diagram of the synchronously rotating frame is illustrated in Fig.1. The RSM can be started asynchronously, and be operated synchronously at steady

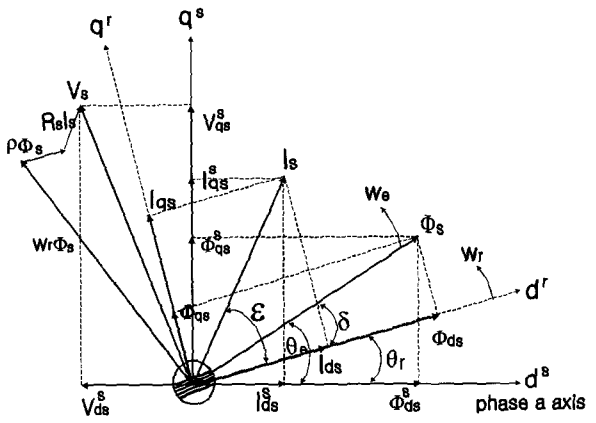

Fig. 1 Vector Diagram of a RSM

state after startup by using proper inverter control. Hence, elimination of both the field winding and damper winding equation forms the basis for the d-q equation for the RSM. The equations are (1)-(5)[3],[4],[7],[12],[13].

$$\begin{bmatrix} V_{ds} \\ V_{qs} \end{bmatrix} = \begin{bmatrix} R_s & 0 \\ 0 & R_s \end{bmatrix} \begin{bmatrix} I_{ds} \\ I_{qs} \end{bmatrix} + \begin{bmatrix} -\omega_r & 0 \\ 0 & \omega_r \end{bmatrix} \begin{bmatrix} \Phi_{qs} \\ \Phi_{ds} \end{bmatrix} + \frac{d}{dt} \begin{bmatrix} \Phi_{ds} \\ \Phi_{qs} \end{bmatrix} \quad (1)$$

$$\frac{d\omega_r}{dt} = \frac{1}{J}(T_e - T_L - B\omega_r) \quad (2)$$

$$\begin{aligned} T_e &= \left(\frac{3}{2}\right)\left(\frac{P}{2}\right)\left(\Phi_{ds} I_{qs} - \Phi_{qs} I_{ds}\right) \\ &= \left(\frac{3}{2}\right)\left(\frac{P}{2}\right) L_d \left(1 - \frac{L_q}{L_d}\right) I_{ds} I_{qs} \\ &= \left(\frac{3}{2}\right)\left(\frac{P}{2}\right)\left(L_d - L_q\right) I_s \frac{\sin(2\varepsilon)}{2} \\ &= \left(\frac{3}{2}\right)\left(\frac{P}{2}\right)\frac{\left(L_d - L_q\right)}{L_d L_q} \Phi_x^2 \sin(2\delta) \end{aligned} \quad (3)$$

$$\begin{bmatrix}\Phi_{ds}\\ \Phi_{qs}\end{bmatrix}=\begin{bmatrix}L_{ls}+L_{md} & 0\\ 0 & L_{ls}+L_{md}\end{bmatrix}\begin{bmatrix}I_{ds}\\ I_{qs}\end{bmatrix}=\begin{bmatrix}L_dI_{ds}\\ L_qI_{qs}\end{bmatrix} \quad (4)$$

$$|\Phi_s|=\sqrt{\Phi_{ds}^2+\Phi_{qs}^2} \quad (5)$$

Where L_{md}, L_{mq} and L_{ls} are, respectively, the direct axis and the quadrature axis magnetizing inductances and the leakage inductance, the quantity R_s is the stator resistance per phase and ω_r is the speed of the rotor.

From (3), we know that the electromagnetic torque can be expressed in terms of the stator current amplitude and current angle ε. This means that torque control dynamics can be maintained by adjusting the flux for optimal efficiency. This is because the flux linkage in the RSM is directly proportional to the stator currents since the rotor circuit is opened [1]-[4].

The equations are simply compared to induction machines because the field winding is nonexistent and the rotor cage is normally omitted. This predicts that the control scheme of the RSM can be simpler than those of synchronous or induction machines.

The inductances are a nonlinear function of rotor position and current and have to be compensated for due to magnetic saturation. In order to measure nonlinear inductance, we measured the inductance versus the stator current and the rotor position angle. Fig.2 shows the measured inductance versus the position and the current. Fig. 3 shows measured L_d and L_q versus the stator current.

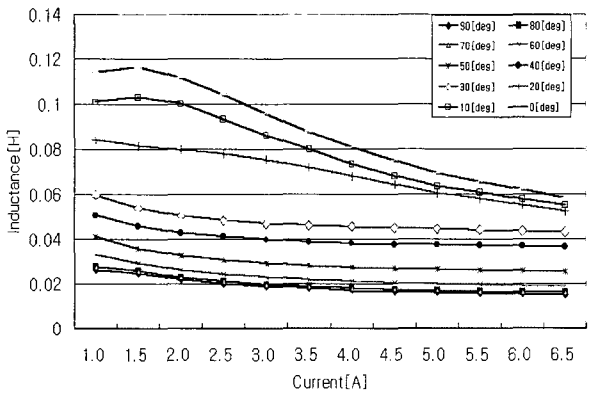

Fig. 2 Measured inductance versus position angle

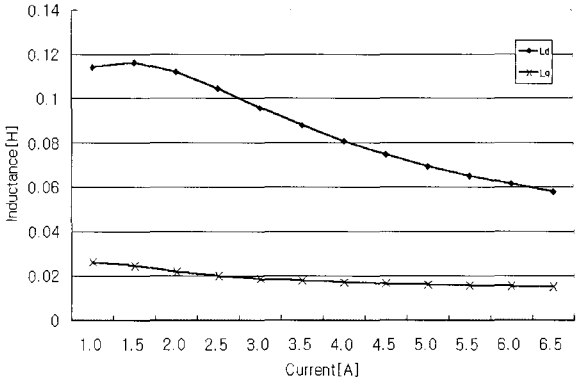

Fig. 3 Measured Ld and Lq versus stator current

3. High performance control

3.1 Mathematical analysis

Fig. 4 shows the d and q-axis equivalent circuit of the RSM in the synchronously rotating reference frame. The resistance R_s represents copper loss. The resistance R_m which accounts for core loss is connected in parallel with the magnetizing branch and induced speed voltage. The current components which are directly responsible for torque and flux production are I_{do}, I_{qo}. These currents differ from the terminal current I_{ds}, I_{qs} because of the existence of core loss branch. From Fig. 4, the d-q voltage equations in the synchronously rotating reference fram for RSM are (6) and (7).

$$\begin{aligned}V_{ds}&=R_sI_{ds}+\frac{d}{dt}L_dI_{do}-\omega_rL_qI_{qo}\\ V_{qs}&=R_sI_{qs}+\frac{d}{dt}L_qI_{qo}+\omega_rL_dI_{do}\end{aligned} \quad (6)$$

$$\begin{aligned}I_{do}&=I_{ds}-I_{dm}\\ &=I_{ds}-\frac{1}{R_m}\left(\frac{d}{dt}(L_dI_{do})-\omega_eL_qI_{qo}\right)\\ I_{qo}&=I_{qs}-I_{qm}\\ &=I_{qs}-\frac{1}{R_m}\left(\frac{d}{dt}(L_qI_{qo})+\omega_eL_dI_{do}\right)\end{aligned} \quad (7)$$

where, L_d, L_q are respectively direct axis inductance and quadrature axis inductance, respectively. Equation (8) is electromagnetic torque considered core loss as

$$T_e = (3/2)(P/2)(L_d - L_q) I_{do} I_{qo} \tag{8}$$

where, P is the number of the poles.

As mentioned previously, the efficiency of a variable speed drive is one of the most important factors. It is possible to compute the copper and the iron losses as a function of I_{do}, I_{qo} , as in (9), (10).

Copper loss :

$$\begin{aligned} P_{co} &= \frac{3}{2} R_s (I_{ds}^2 + I_{qs}^2) \\ &= \frac{3}{2} R_s \left\{ (I_{do} - \frac{\omega_e L_q I_{qo}}{R_m})^2 + (I_{qo} + \frac{\omega_e L_d I_{do}}{R_m})^2 \right\} \end{aligned} \tag{9}$$

Iron loss :

$$\begin{aligned} P_{ir} &= \frac{3}{2} R_m (I_{dm}^2 + I_{qm}^2) \\ &= \frac{3}{2} R_m \left\{ (\frac{\omega_e L_q I_{qo}}{R_m})^2 + (\frac{\omega_e L_d I_{do}}{R_m})^2 \right\} \end{aligned} \tag{10}$$

The losses are concentrated in the stator Those losses in the rotor, which are mainly due to flux ripple, are assumed to be negligible. The efficiency is optimized by minimizing the total losses of copper and iron losses. Let the ration of d- and q-axis current be $\zeta = I_{qo} / I_{do}$, the optimal ratio minimizing the total losses can be found for a given speed and load condition by (11). In the calculation of (11), the generated torque must be constant for the given operation point as (12).

$$\partial P_{total} / \partial \zeta = 0 \tag{11}$$

$$I_{do} I_{qo} = \text{constant} \tag{12}$$

By solving (11) and (12), the optimal ratio of torque producing current $\zeta_{optimal}$ can be found as (13)

$$\zeta_{optimal} = \sqrt{\frac{R_s R_m^2 + (R_s + R_m)(\omega_e L_d)^2}{R_s R_m^2 + (R_s + R_m)(\omega_e L_q)^2}} \tag{13}$$

The reference flux is calculated from current angle(ε)and current vector(I_s) as (14)

$$|\Phi_s^*| = I_s \sqrt{L_q^2 \sin^2 \varepsilon + L_d^2 \cos^2 \varepsilon} \tag{14}$$

Thus, to minimize loss, the $\zeta_{optimal}$ is constant at a given speed and depends on only the motor parameters and motor speed. Therefore, a RSM drive can achieve high performance using a simple control algorithm.

3.2 Neural Network

In this paper, a NN is utilized to map eq.(14). Fig. 5 shows the configuration of the NN used in the proposed algorithm. This NN consists of 2 input nodes(stator current and current angle), 6 hidden layers and 3 outputs(flux reference and inductances). Nodes in the hidden layer and output layer have the sigmoid function. The back propagation(BP) rule to train the NN is used. The off-line training of the network is performed to update the weights[2].

3.3 Flux Observer

The most important part of DTC is the control of the amplitude and rotating speed of the stator flux linkage. The calculation of stator flux is then very important. One of the best and simplest calculation methods, which is accurate over a wide range of speeds, is to calculator the stator flux from the stator current, voltage and estimated rotor angle. Fig. 6 shows.

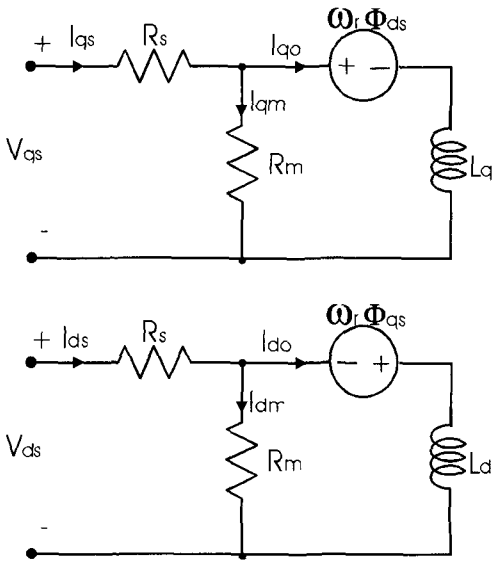

Fig. 4 Equivalent circuit of a RSM with core loss

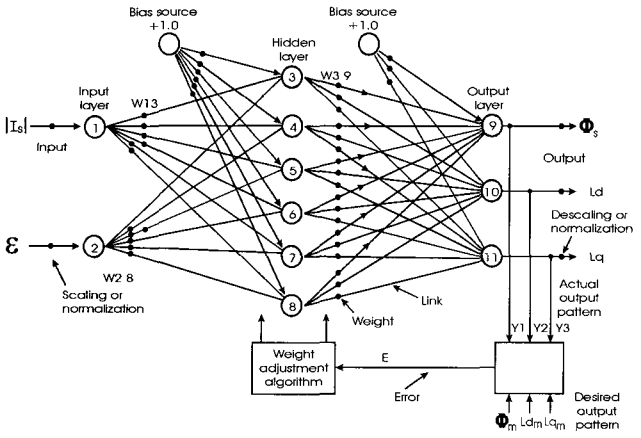

Fig. 5 Configuration of the neural network

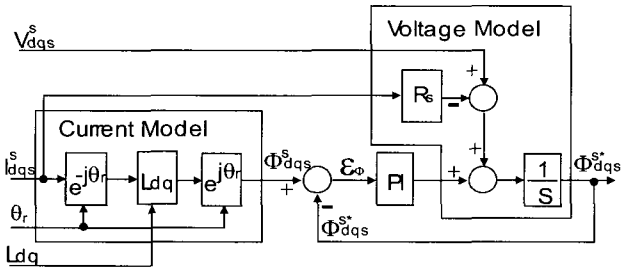

Fig. 6 Closed loop flux observer

such a closed-loop, stationary frame observer, which is hereafter described as the "closed-loop flux observer". A closed-loop flux observer is globally stable in a stationary frame and works over a wide range of speeds. The stator flux-linkage in the stator reference frame is Eq. (19).

$$\begin{bmatrix} I_{dr}^{s} \\ I_{qr}^{s} \end{bmatrix} = \begin{bmatrix} \cos\theta_r & \sin\theta_r \\ -\sin\theta_r & \cos\theta_r \end{bmatrix} \begin{bmatrix} I_{ds}^{s} \\ I_{qs}^{s} \end{bmatrix} \tag{15}$$

$$\begin{bmatrix} \Phi_{dr}^{s} \\ \Phi_{qr}^{s} \end{bmatrix} = \begin{bmatrix} I_{dr}^{s} \cdot Ld \\ I_{qr}^{s} \cdot Lq \end{bmatrix} \tag{16}$$

$$\begin{bmatrix} \Phi_{ds\_CM}^{s} \\ \Phi_{qs\_CM}^{s} \end{bmatrix} = \begin{bmatrix} \cos\theta_r & \sin\theta_r \\ -\sin\theta_r & \cos\theta_r \end{bmatrix} \begin{bmatrix} \Phi_{dr}^{s} \\ \Phi_{qr}^{s} \end{bmatrix} \tag{17}$$

$$\varepsilon_{\Phi} = \Phi_{dqs\_CM}^{s} - \Phi_{dqs}^{s*} \tag{18}$$

$$\Phi_{dqs}^{s*} = \int[(V_{dqs}^{s} - R_s \cdot I_{dqs}^{s}) + \varepsilon_{\Phi}(K_1 + \frac{K_2}{P})]dt \tag{19}$$

Where, I_{dqs}^{s} represents the stator current, I_{dqr}^{s} represents the current, Φ_{dqs}^{s} represents the stator flux-linkage, Φ_{dqr}^{s} represents the rotor flux-linkage.

4. Direct torque control of RSM

The two methods of DTC of a RSM are the constant flux method and the variable flux method. A DTC algorithm is able to control the stator flux linkage and the electromagnetic torque directly by selecting the optimum inverter switching pattern. The switching pattern is selected to restrict the flux and torque errors within the respective flux and torque hysteresis bands, and to obtain fast torque response, low switching frequency, and low harmonic losses. DTC allows very fast torque response and flexible control of the RSM. The main advantages of DTC are: the absence of coordinate transformations and voltage decoupling blocks; a reduction in the number of controllers; and resistance to motor parameter variations. Additionally, the actual flux-linkage vector position and flux linkage sector do not have to be determined [1],[12],[13].

5. System configuration

Fig.7 shows the applied system configuration. The control system consists of an IGBT voltage source inverter(VSI), a stator flux observer, two hysteresis controllers, a neural network, an optimal switching look-up table, and a TMS320C31 DSP controller using fully integrated control software. In order to remunerate nonlinear inductance, the values of L_d and L_q are used to compensate against d-axis and q-axis current. The neural network controls the reference flux so that the current remains at the optimum angle to assure optimum efficiency. Table 1 shows the applied motor parameters. Fig. 8 shows a photo of the applied RSM with a flux barrier rotor.

Table 1 Applied motor parameters

Inertia moment	0.003	Rs	1.0[Ω]
Poles of stator	4	Rated torque	4.0[Nm]
Poles of rotor	4	Rated current	5.0[A]
Rated output	1.0[kW]	Lq	28[mH]
Rated speed	2400[rpm]	Ld	72[mH]

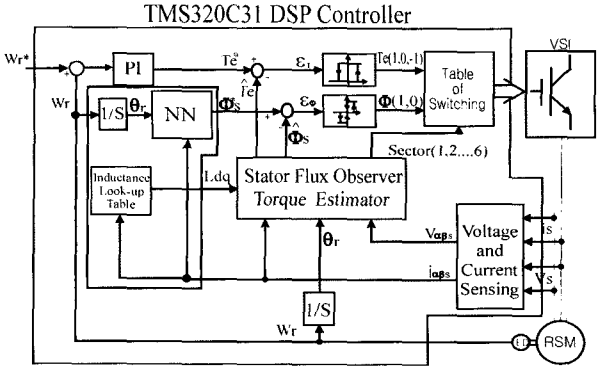

Fig. 7 System configuration

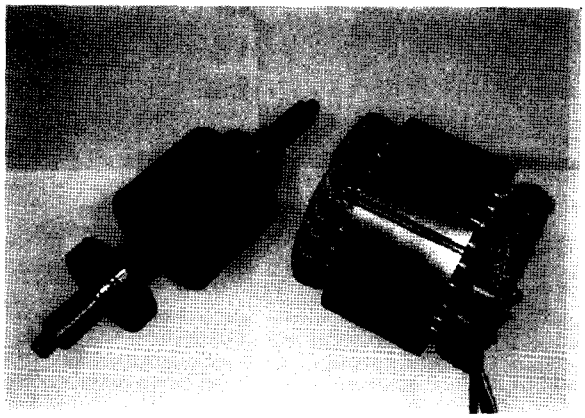

Fig. 8 A Model of the Reluctance Synchronous Motor

6. Experimental results

In this paper, we carried out an experimental study of direct torque control of a RSM using a neural network to obtain high performance. In order to obtain optimum efficiency, the optimum current angle was mathematically calculated and sent to the RSM. Fig. 9 shows static efficiency versus torque characteristics for both the conventional constant flux control and our proposed control at various speeds. Our proposed method proves to be much more efficient than the conventional method under light load conditions.

Figs. 10 and 11 show the dynamic characteristics of constant flux control and our proposed control. In these figures, the speed command is changed by 1000 to -1000[rpm]. Fig.10(a) represents the characteristics of speed response using constant flux control and Fig.10(b) represents the waveform of the stator flux linkage using constant flux control. Fig.11(a) shows the characteristics

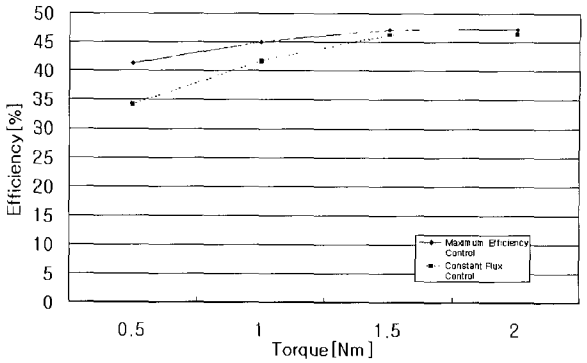

(a) Efficiency characteristics at 300[rpm]

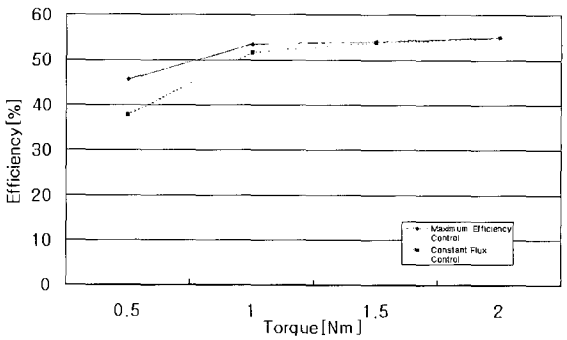

(b) Efficiency characteristics at 500[rpm]

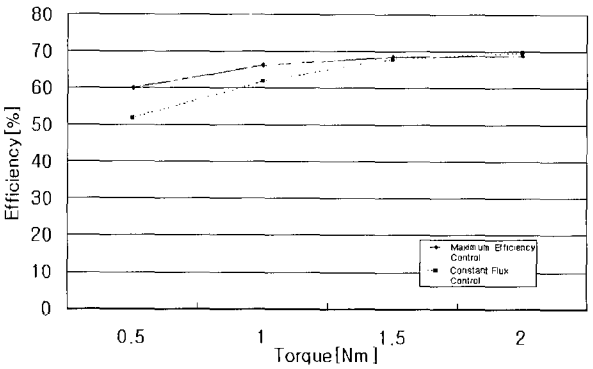

(c) Efficiency characteristics at 1000[rpm]

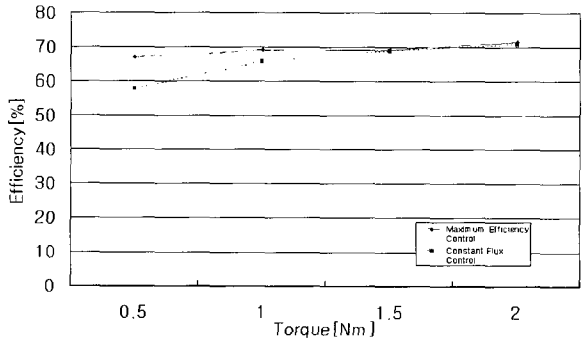

(d) Efficiency characteristics at 1500[rpm]

Fig. 9 Efficiency characteristics versus control method

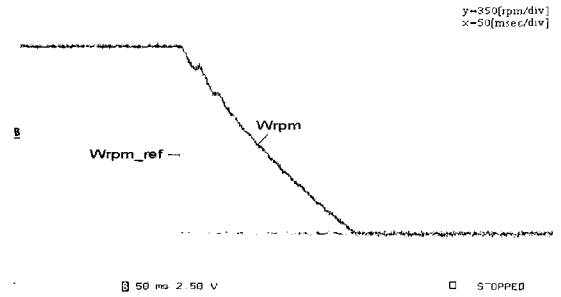

(a) Characteristics of speed response

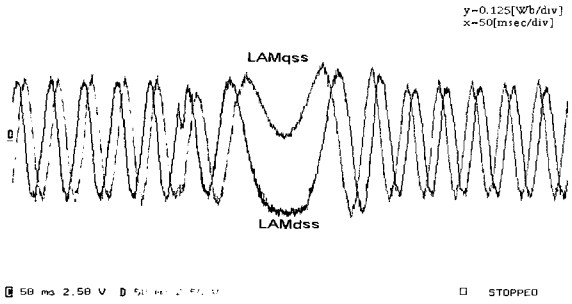

(b) Waveform of stator flux linkage

Fig. 10 Control characteristics of constant flux control

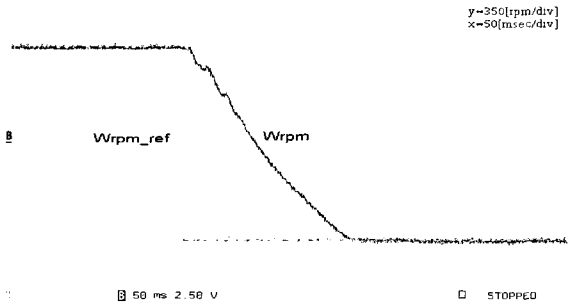

(a) Characteristics of speed response

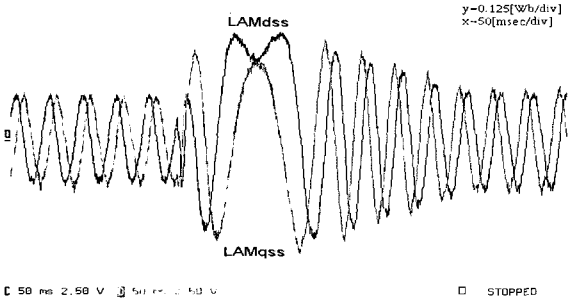

(b) Waveform of stator flux linkage

Fig. 11 Control characteristics of efficiency optimized control

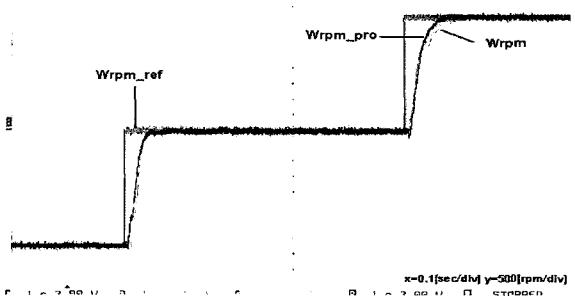

(a) Comparison of speed response

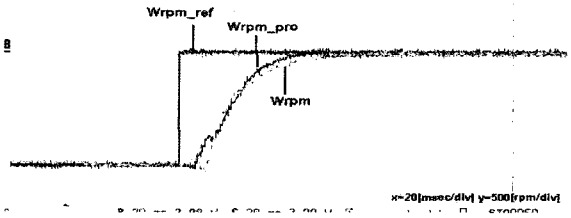

(b) Enlarged speed response in transient state

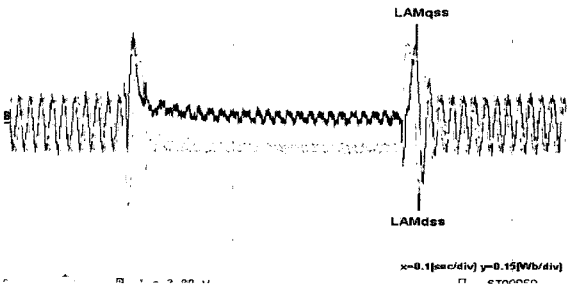

(c) Waveform of stator flux linkage under proposed method

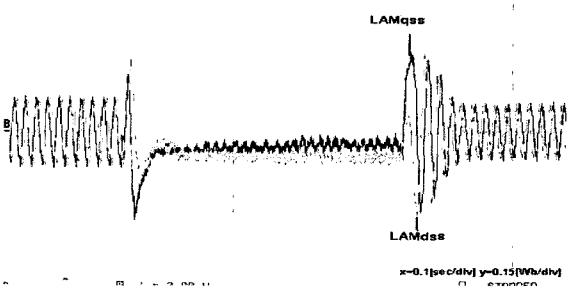

(d) Waveform of stator flux linkage under control method which flux is proportional to torque

Fig. 12 Control characteristics of efficiency optimized control

of speed response using our proposed control and Fig.11 (b) shows the waveform of the stator flux linkage using our proposed control. In steady state, the flux values are minimized using our proposed control method as compared to the constant flux control method. This minimizes machine efficiency losses.

Fig. 12 shows the dynamic characteristics of the constant flux control algorithm, which maintains the flux proportional to torque, and our proposed control algorithm. In this figure, speed command is varied from -1500 to 0 and 1500[rpm]. Fig.12(a) represents a comparison of the speed response. And Fig.12(b) represents the enlarged characteristics in the transient state. As one can see, the proposed control algorithm which uses a NN performs better than the constant flux control algorithm. Fig.12 (c) represents the waveform of the stator flux linkage under the proposed method and Fig.12(d) represents the waveform of the stator flux linkage under the constant flux method.

7. Conclusions

For a reluctance synchronous motor, torque dynamics can be maintained by controlling the flux level because the generated flux is directly proportional to the stator current. In this paper, to minimize the efficiency loss of the machines and obtain good dynamic response, the stator flux command which maintained optimum current angle is derived based on an equivalent circuit model of the machine. The NN is trained off-line to map the optimal flux reference. To validate the performance of the proposed method, we carried out experiments with a 1.0[kW] flux barrier reluctance synchronous motor. Experimental results show that the proposed control algorithm allows machine efficiency losses at variable operating points to be reduced while maintaining good dynamic response.

This research was supported by the Yeungnam College of Science & Technology Research Grants in 2004.

References

[1] Peter Vas, Sensorless Vector and Direct Torque Control, Oxford Press, 1998.

[2] Bimal K. Bose, Modern Power Electronics and AC Drives. Prentice Hall PRT, 2002.

[3] Iron Boldea, Reluctance Synchronous Machines and Drives, Oxford Science, 1996.

[4] T. Matsuo, and T. A. Lipo, "Field Oriented Control of Synchronous Reluctance Machine," in Proc. PESC.1993.

[5] Hyeoun-Dong Lee, Seog-Joo Kang, and Seung-Ki Sul, "Efficiency-Optimized Direct Torque Control of Synchronous Reluctance Motor using Feedback Linearization, " IEEE Trans. on IE, Vol. 46, No. 1, pp. 192-198, Feb. 1999.

[6] H. Murakami, Y. Honda, S. Morimoto, and Y. Takeda, "Performance Evaluation of Synchronous Reluctance Motor and the Order motors with the Same Distributed Winding and Stator Configuration," T.IEEE Japan, Vol. 120-D, No.8/9, pp. 1062-1074, 2000.

[7] A. Vagati, and T. A. Lipo, "Synchronous Reluctance Motors and Drives : A New Alternatives," IEEE Industry Application Society Annual Meeting Tutorial, 1994.

[8] R. E. Betz, R. Lagerquist, M. Jovanovic, and T. J.E. Miller, "Control of Synchronous Reluctance Machines," IEEE Transactions on Industry Applications, vol. 29, no. 6, November/December, pp. 1110~1121, 1993.

[9] Seog-Joo Kang, and Seung-Ki Sul "Efficiency Optimized Vector Control of Synchronous Reluctance Motor." IAS '96., Vol. 1, pp. 117-121, 1996.

[10] W. L. Soong, D. A. Staton, and T. J. E. Miller, "Validation of Lumped-Circuit and Finite-Element Modeling of Axially-Laminated Brushless Motors," IEEE Conference on Electrical Machines and Drives, pp. 85~90, 1993.

[11] Min-Huei Kim, Nam-Hun Kim, Min-Ho Kim, and Dong-Hee Kim, "An Induction Motor Position Control System with Direct Torque Control", Proceedings of the ISIE 2001, pp. 771~774, June, 2001.

[12] A. Kilthau, and J.M. Pacas, "Sensorless Control of the Synchronous Reluctance Machine", JPE, Vol. 2, No. 4, pp3 95-103, April, 2002.

[13] Min-Huei Kim, Nam-Hun Kim, Dong-Hee Kim, Shigeru Okuma, and James C. Hung, "A Position Sensorless Motion Control System of Reluctance Synchronous Motor with Direct Torque Control", ISIE 2002, pp.1148-1153, 2002.

[14] Hamid A. Toliyat, and Steven Campbell, DSP-Based Electromechanical Motion Control, CRC press, 2004.

Min-Huei Kim was born in Kyengbuk Province, Korea on August 25, 1951. He received the B.S. and the M.S. degree from Yeungnam University, Kyeungbuk, Korea, and the Ph.D. degree from the University of Chung-Ang, Seoul, Korea, all in electrical engineering, in 1974, 1980, and 1989, respectively. He has worked in Research and Development for electric motor design of the Shinil Industrial Company from 1977 to 1978 in Seoul, Korea, In 1978, he was hired as an instructor at Yeungnam Junior College, Daegu, Korea. He became an Assistant Professor, Associate Professor and Professor in 1981, 1987, 1992, respectively. From 1993 to 1995, he was a Visiting Research Professor at the Power Electronics Application Center (PEAC) at The University of Tennessee, Knoxville, USA. He is currently a professor in the Department of Electrical Automatic Engineering at Yeungnam College of Science and Technology, Daegu, Korea. His research interests are control systems of motor drives, power converters, neural networks and their application to power electronics. He is a member of the KIPE and JIEE, a life member of KIEE, and a senior member of IEEE.